Monolayer Conveyor for Stably Trapping and Transporting Sub-1 nm Particles

*Mohammad Danesh, Mehdi Jafary Zadeh, Tianhang Zhang, Xiaohe Zhang, Bing Gu, Jin-Sheng Lu, Tun Cao, Zhengtong Liu, Andrew T. S. Wee, Min Qiu, Qiaoliang Bao, Stefan Maier, and Cheng-Wei Qiu**

Efficient manipulation of nanoparticles and single molecules has always been of great interest and potential in nanotechnology. However, many challenges still remain in effectively functionalizing structures for this purpose. In this work, taking advantage of graphene's Dirac plasmon for its extreme confinement and tunability, a monolayer conveyor along which the position of optical potential well can be dynamically controlled is theoretically proposed. It is shown that by tuning a single voltage, one can manipulate the resonance along the graphene nanoribbon by changing graphene's effective surface plasmons wavelength. A configuration of monolayer graphene conveyor is proposed and Langevin dynamics reveals that a prototypical nanoparticle (1 nm size) can be effectively confined and transported along the device with proper external bias voltage. Hence, this work successfully proposes a promising avenue toward reconfigurable nanomanipulation of sub-1 nm nanoparticles, and goes beyond the current state-of-the-art of optical micrometer/nanometer-sized particles manipulation with optical tweezers and nanoplasmonic tweezers.

1. Introduction

During the last few decades, manipulations of micrometer-scale objects with light have been demonstrated in large numbers and go on attracting great interests. For example, by exploiting the competition of two kinds of light-induced forces, optical force and photophoretic force, a gold microplate can be driven to move back-and-forth on a tapered fiber.[1] Besides, photophoretic force can be utilized independently to transfer gold-coated hollow glass microspheres along a radially or azimuthally polarized beam in a long range.[2] Conventional optical tweezers have been developed into a widely adopted tool for trapping and manipulating micrometer sized objects.[3-8] These tweezers have been used in atomic cooling,[5] trapping bacteria,[7] assembly

Dr. M. Danesh, Prof. T. Zhang, Prof. C.-W. Qiu
Department of Electrical and Computer Engineering
National University of Singapore
Singapore 117583, Singapore
E-mail: chengwei.qiu@nus.edu.sg

Dr. M. Danesh
Transcelestial Technologies
Singapore 058573, Singapore

Prof. M. J. Zadeh, Prof. Z. Liu
Institute of High Performance Computing (A*STAR)
Singapore 138632, Singapore

Prof. T. Zhang, Prof. A. T. S. Wee, Prof. C.-W. Qiu
Graduate School for Integrative Sciences and Engineering
National University of Singapore
Centre for Life Sciences (CeLS)
Singapore 117456, Singapore

Dr. X. Zhang, Prof. B. Gu
Southeast University
Nanjing 210096, China

Prof. J.-S. Lu
State Key Laboratory of Modern Optical Instrumentation
College of Optical Science and Engineering
Zhejiang University
Hangzhou 310027, China

Prof. T. Cao
Department of Biomedical Engineering
Dalian University of Technology
Dalian 116024, China

Prof. A. T. S. Wee
Department of Physics
National University of Singapore
Singapore 117542, Singapore

Prof. M. Qiu
Institute of Advanced Technology
Westlake Institute for Advanced Study
Westlake University
Hangzhou 310024, China

Prof. Q. Bao
Department of Materials Science and Engineering, and ARC Centre of Excellence in Future Low-Energy Electronics Technologies (FLEET)
Monash University
Victoria 3800, Australia

Prof. S. Maier
Chair in Hybrid Nanosystems
Faculty of Physics
Ludwig-Maximilians-Universität München
München 80799, Germany

The ORCID identification number(s) for the author(s) of this article can be found under https://doi.org/10.1002/lpor.202000030

DOI: 10.1002/lpor.202000030

of nanowires[9,10] and even creating fields that can exert negative optical forces.[11-14] However, these applications have been mostly limited to particles in the micrometer scale. When dealing with objects in the nanometer scale, both ways using photophoretic force and optical force (i.e., conventional optical tweezers) face major challenges. It is owing to that, for photophoretic force, it is dependent on the temperature gradient while creating a considerable temperature gradient in nanometer scale is extremely hard. For optical force, this force exerted on a nanoparticle is extremely small due to the diffraction limit.[15-18] In addition, the small surface area of the nanoparticle reduces the drag forces, making the nanoparticles more susceptible to random thermal fluctuations.[18]

In order to increase the exerted optical forces on nanoparticles, the interaction between light and metals has been applied to excite surface plasmons[19] which are usually associated with enhanced evanescent near-field components to produce remarkable gradient forces and effectively maneuver these nanoparticles.[17-19] Plasmonic tweezers in the last few years have allowed us to trap objects from the micrometer range down to the nanoscale. For example, polystyrene nanoparticles ranging from 200,[20] 110,[21] and 20 nm[22,23] in diameter were trapped efficiently in experiments using plasmonic nanostructures of nanoantennas,[20] nanopillars,[21] nanocavities,[22] and nanoholes.[23] Theoretical studies have also demonstrated efficient trapping mechanisms for particles as small as 10 nm within slot waveguides,[24] hybrid plasmonic waveguides,[25] graphene plasmons,[26] gold nanogap electrodes,[27] and even 2 nm particles using the tip of a tapered coaxial waveguide.[28] However, controllable trapping and functionalization of sub-1 nm particles or in other words atomic and molecular scale nanomanipulation still face considerable challenges.

In addition to scaling toward smaller sized particles, various new optical tweezer functions for nanoparticles have also been achieved such as sorting,[29-32] transportation,[33-36] rotation,[37] and positioning[38,39] using different techniques such as polarization control,[40] frequency control,[33,34] Fano resonance induced optical forces,[31,41] and power control.[29] Nevertheless, significant challenges have yet to be overcome. For example, the long-range mobilization of nanoparticles require mechanical movements of the physical tweezer setup, as well as the change of frequency or polarization of the illumination, or the amplitude/phase of the structured light, which are difficult to implement in integrated applications for sub-10 nm sized particles.[29,33,34,40]

These aforementioned limitations stem from the nature of the material used in classic nanoplasmonic tweezing such as gold and silver, since the electromagnetic properties of these materials are not easily tunable. In other words, once the trapping structure is fabricated, it can be quite challenging to modify the effective optical potentials. To this end, Dirac plasmons in graphene[42-47] offer us a new tool since it allows a wide tuning range of the effective electromagnetic properties via electrostatic screening.[45,46,48,49] There have already been preliminary studies of the properties of forces mediated by graphene plasmons.[50-53] For example, a graphene sheet placed on top of a reflective substrate can be used to create a self-levitating sheet,[50] and a graphene waveguide can be used to create a strong nanoparticle trap inside the waveguide.[51]

Our work focuses on utilizing the main advantages and uniqueness of graphene plasmons, i.e., its tunability and strong electromagnetic field enhancement,[43] to create a novel solution for sub-nanometer nanoparticle manipulation: a molecular nanoconveyor platform. We propose a simple yet novel design that can be used to create an electrically tunable optical potential field. This optical potential field can be used not only to trap but also to control the position of the nanoparticles along the edges of the structure, i.e., a graphene conveying belt, by altering an electrical voltage of the back gate to yield full control over the position of the particle and even its transportation speed along the optical nanoconveyor. To verify the validity of our postulations under realistic conditions, we used C_{60} admolecule as prototype molecule and investigate its diffusive and drift motion on graphene under applied external field using Langevin dynamics (LD) with parameters carefully obtained from molecular dynamics and thermal simulations.[54] Organic molecules physisorbed on graphene are important in a variety of technologies.[55,56] Such intriguing potential applications clearly mark the importance of constructing a physical manipulation platform for the advanced control of the mobility of buckyballs and other organic molecules in various environments including on membranes and surfaces.[54,57-62]

The schematic of our design is illustrated in **Figure 1**. The excitation of localized surface plasmon resonances (LSPR) on the graphene surface can be achieved using a normal-incident plane wave. The substrates are made of a nonabsorption material. To transport the molecules along the graphene ribbon edge, at the first step, we need the molecules to be tightly trapped at the edge. Consequently, we can control the position in the x-direction (marked in Figure 1) by applying a tunable optical force on the molecules along this direction. The graphene nanoconveyor is designed in a tapered manner to achieve this x-directed optical force. The slightly tapered design introduces asymmetry in the x direction, creating electric field inhomogeneity along the nanoconveyor, resulting in optical gradient forces. One of the important characteristics of LSPR is their extreme sensitivity to geometrical dimensions. Therefore, the exact location of the geometric resonance occurring on the tapered nanoconveyor depends on λ_{sp}, the effective wavelength of the surface plasmon. Due to graphene's unique Dirac plasmons, the surface plasmon wavelength can be directly tuned by changing the carrier density via an electrical back gate. Therefore, by changing the voltage of the back gate, the carrier density changes, varying λ_{sp} and resulting in the geometrically sensitive LSPR resonance that can be reallocated at different locations along the nanoconveyor as plotted in the inset of Figure 1. The time domain transfer dynamics of fullerene C_{60} across graphene nanoconveyor is also plotted in the inset, while this part will be discussed later.

In order to demonstrate the concept of an electrically tunable optical potential, we carefully design a tapered graphene ribbon in vacuum environment at room temperature (300 °K) (see **Figure 2**a). The tapered ribbon can act as a graphene nanoconveyor allowing the geometrically sensitive localized surface plasmon resonances to shift along its length. In this design, the nanoconveyor l is 1.5 μm long and the width gradually changes from $w_1 = 100$ nm to $w_2 = 80$ nm. It should be noted that graphene's broadband mid-infrared plasmons allow these dimensions to be geometrically scaled by changing either the operating wavelength λ_0 or the doping range $E_{F1} < E_F < E_{F2}$, depending on the

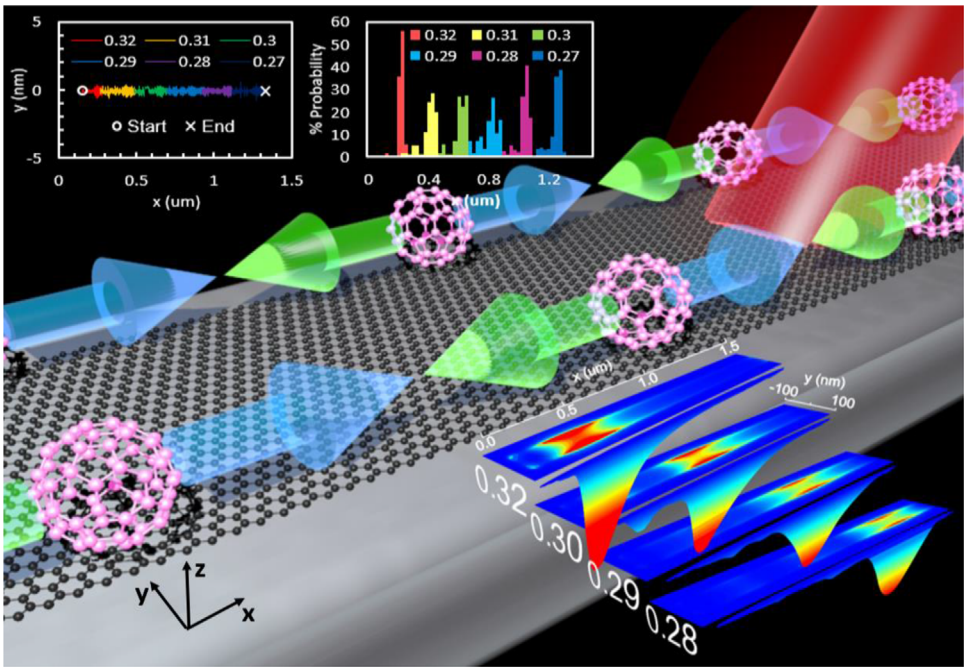

Figure 1. Schematic of sub-1 nm graphene nanoconveyor. The resonance area along the graphene nanoribbon could be manipulated by tuning a single voltage. C_{60} molecules could be transported bidirectionally along the edges of the nanoribbon with the shift of resonance area, realizing a nanoconveyor.

geometrical requirements. The structure is optimized to operate with a Fermi Level of $0.27\,\text{eV} < E_F(\text{V}) < 0.32\,\text{eV}$, which is very practical. In our case, we have designed the nanoconveyor to operate at the wavelength of commercially available CO_2 lasers. The incident laser has a wavelength of $\lambda_0 = 10.7\ \mu\text{m}$ and the incident intensity is 100 mW μm^{-2}. The light propagates normally onto the graphene surface (z-direction) and is linearly polarized with its polarization along the width of the nanoconveyor, creating localized plasmon resonances on the edges of graphene structure.[63] The plasmon mode is the dipole like resonance mode along the narrow side of the ribbon, which moves along the ribbon as the Fermi level changes. These plasmon hotspots can be observed in Figure 2a for the case of a Fermi level of $E_f = 0.30$ eV. Note that the electric field intensity plot has been scaled to fit within the graphical design.

The highly confined electromagnetic near-fields are due to geometrical LSPRs, causing electric charges to be disposed at the two edges of the graphene nanoconveyor, which gives rise to a highly resonant electrical dipole mode that results in drastically changing evanescent fields E_{lspr}. These near-fields could have electromagnetic energy enhancements as high as $|E_{\text{lspr}}/E_0|^2 > 10^4$. The enhanced evanescent fields are also extremely confined in spatial dimensions in orders as small as $\delta l \propto 10$ nm, resulting in huge electric nearfield spatial gradients. Spatial gradients of electric amplitude create optical gradient forces that serve to pull nanoparticles toward regions with maximum potential, potentially leading them to become optically trapped. As the size of the fullerene C_{60} molecules are of the order of ≈ 1 nm—orders of magnitude smaller than the wavelength of the incident laser—the Rayleigh regime is assumed. Thereby we can directly relate the optical forces to the gradient fields $\mathbf{F}_{\text{gra}} \propto \nabla|\mathbf{E}_{\text{lspr}}|^2$ which can trap particles in very tightly optical potentials $\mathbf{U}_{\text{gra}} \propto |\mathbf{E}_{\text{lspr}}|^2$. Once a nanoparticle is in the vicinity of these optical potentials, it will be subject to large forces until it is trapped into the minimum energy point. In other words, the plasmons generated by the graphene nanoribbon could have resolution as high as nanometer scale. Generally, an optical trapping with potential depth lager than one $k_B T$ can be regarded as stable.[64] When the Fermi level is in the range of $0.27\ \text{eV} < E_F(\text{V}) < 0.32$ eV, the potential generated by the LSPR of graphene is $\approx 10^4$ times larger than that generated by incident field $\mathbf{U}_{\text{gra}}/\mathbf{U}_0$, indicating that the potential is large enough to trap nanoparticles.

We perform full-wave electromagnetic simulations (see Section S2 in the Supporting Information) to calculate the forces and optical potentials at the lower edge of the graphene ribbon, while the case of upper edge will be very similar. For an example, at the doping level of 0.32 eV (Figure 2b,c), LSPR is generated at the broader end of the nanoconveyor. The electromagnetic near-fields at this region lead to strong gradient optical forces there, creating a 3D optical potential centered at x_m (0.32 eV) = 250 nm on the edges of the nanoribbon. The optical forces in the horizontal (lateral) planes as in Figure 2b,c are calculated when a fullerene C_{60} molecule is placed with its center of mass 0.8 nm above the graphene sheet. The x and y directions here are defined as the directions parallel and perpendicular to the lower edge of the graphene ribbon, respectively. A closer look at the in-plane optical forces F_x, and F_y shows a major difference between them. The force in the y-direction is nearly two orders larger than F_x. The reason is that the electric field in the y direction is much more confined than in the x direction. Thus, the molecules could be trapped into a thin line at the proximity of the graphene edges.

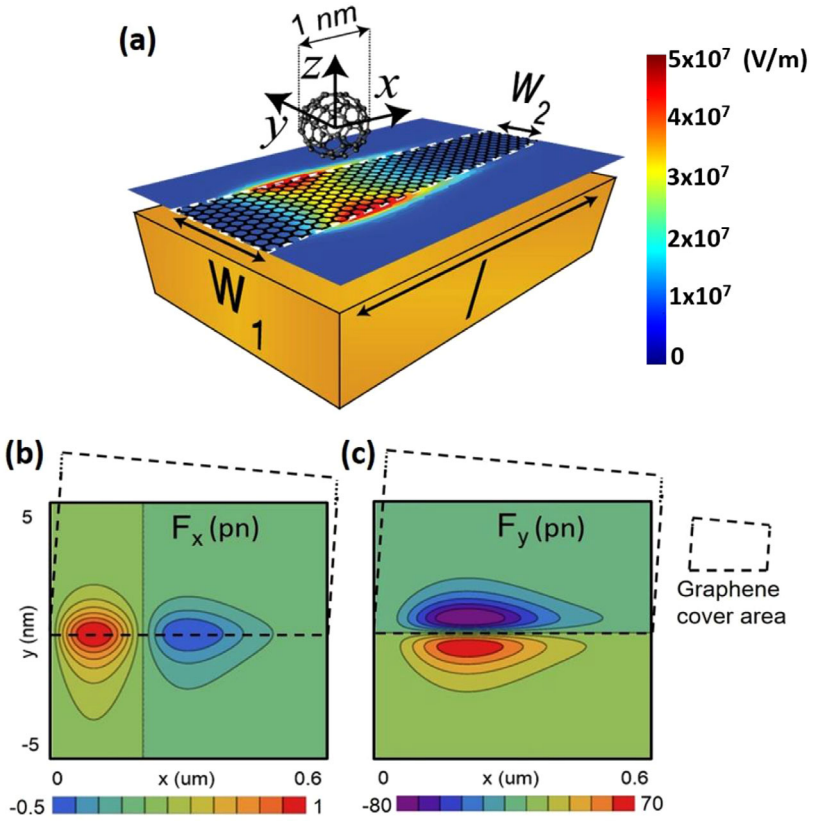

Figure 2. a) Structure of the graphene optical nanoconveyor. The electric field is assumed to be propagating normally onto the graphene surface with a polarization along the width of the nanoconveyor, resulting in a localized plasmon resonance on the graphene structure. b,c) Optical force fields calculated near the lower edge of the graphene ribbon. The *x* and *y* directions here are defined as the directions parallel and perpendicular to the lower edge of graphene ribbon, respectively. The area enclosed by dashed lines represent the graphene covered area which is in tapered shape. b) F_x optical force in the transport direction along the edge, i.e., *x* direction. c) F_y created perpendicular to the transport direction.

Once the strong *y*-directed forces pull the particles into the nanoconveyor and trap them in the *y*-direction, the particles become closer to the focused near-fields and as a result more susceptible to the long range F_x longitudinal forces. The F_x force on C_{60} ball is quite long-range, extending a few hundred of nanometers along the graphene nanoconveyor, as shown in Figure 2b. The optical force in this case creates a stable trap pulling the particle toward the trapping region at $x_m \propto 250$ nm along the graphene nanoconveyor. As the voltage is changed, the trapping location $x_m \propto E_f \propto \sqrt{V_B}$ can be shifted toward the other end of the nanoconveyor as shown in **Figure 3**. The structure is designed to create a highly focused electromagnetic field that enables a very stiff trap in the *y*-direction effectively confining the particles along a narrow trajectory while it is transported from one side of the nanoconveyor to the other. Trapping stability can be achieved since an optical potential can be obtained in our system ≈10 times larger than the thermal energy ≈10 $k_B T$.[3] The trapping potential and forces in vertical direction are presented in details in Section S3 (Supporting Information).

Figure 3 shows that the optical potential well can be almost linearly shifted along the nanoconveyor *x*-direction by tuning the Fermi level. The graphene's Dirac plasmon dispersion directly relates the effective plasmon wavelength to the level of doping on the graphene structure and induces a longer λ_{sp} for a larger E_F. As mentioned, this allows us to take advantage of geometrically sensitive localized plasmon resonances to create focused electromagnetic energy spots at various locations along the graphene nanoconveyor. Therefore, shifting of the optical potential well by changing of the electrostatic doping is enabled. A linear relation between optical potential peak and Fermi level is found in the form $x_m(\mu m) = aE_F(eV) + b$ (Figure 3b) which also corresponds to the graphene's linear plasmon dispersion.

We further investigate the effects of our designed optical potential with regard to the mobility of the prototypical nanoparticle using Langevin dynamics.[65-67] Using the Langevin equation (LE) for the case of a single absorbed molecule on a surface, all of the substrate degrees of freedom in the equations of motion are coarse-grained and replaced by a random force, i.e., a thermal heat bath, so that only the admolecule's equation of motion remains. Hence, the LE of a free admolecule can be written as the following

$$m\ddot{\mathbf{r}} = -\nabla U(\mathbf{r}) - m\eta\dot{\mathbf{r}} + \xi(t) + \mathbf{F}_{ext}(\mathbf{r}) \quad (1)$$

where m is the mass of the admolecule, $\mathbf{r}$ is the position vector of the admolecule's center-of-mass (COM), $U(\mathbf{r})$ is the potential energy surface[68] of the admolecule/substrate system, η is the

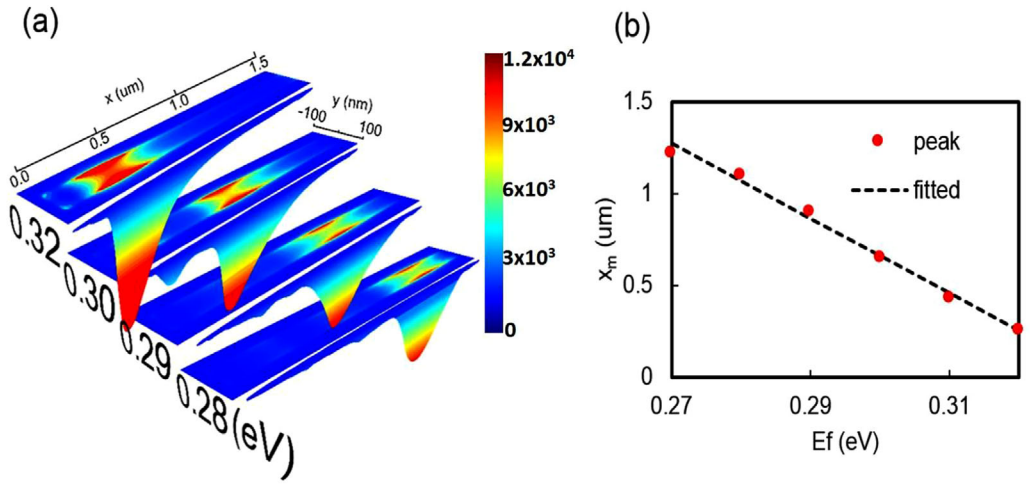

Figure 3. Shifting of optical potential field by changing of electrostatic doping. a) The absolute squared value of the electrical field enhancement $|E/E_0|^2$ created by the graphene nanostructure under various levels of electrostatic doping. For small particles in the Rayleigh regime $|E/E_0|^2$ is directly proportional to the optical potential. b) Peak positions of the optical potentials versus Fermi level of the graphene sheet. A linear relation between optical potential peak and Fermi level is found which corresponds to graphene linear Dirac plasmon dispersion.

friction coefficient between the admolecule and the substrate (details in *S*ection s3 of the Supporting Information), ξ is the stochastic force (heat bath), t is the time, and $\mathbf{F}_{ext}$ is the external force. In this context, the effective stochastic forces from the thermal fluctuation of the substrate atoms (the heat bath), is usually included as a white noise.[67] It is known that the C_{60} admolecule on the pristine graphene at temperatures above 25 K performs a continuous Brownian motion which is independent of the geometry of the PES.[54,60,66] In this Brownian regime of free surface diffusion, the $U(\mathbf{r})$ is negligible and the dynamics of the system is mainly governed by the frictional forces between the admolecule and the substrate.[68] To solve the Langevin model of our system, these frictional forces and their temperature dependence can be adapted from the large-scale molecular dynamics simulations using realistic interatomic potentials (see details in Section S4 of the Supporting Information).

The external force is responsible for applying a drift on the stochastic motion of the admolecule. In the case of applied optical fields, $\mathbf{F}_{ext}$ can be written as

$$\mathbf{F}_{ext}(\mathbf{r}) = \mathbf{F}_{opt}(\mathbf{r}) + \mathbf{F}_{thermal}(\mathbf{r}) \quad (2)$$

where $\mathbf{F}_{opt}$ is the optical (plasmonic) force due to the flux of photon momentum on the nanoparticle, and $\mathbf{F}_{thermal}$ is a force imposed by the thermal gradient which may be formed by the plasmonic losses occurring inside the substrate.[69-71] In this device, the temperature distribution is simulated and shown in the Section S7 (Supporting Information). We found the temperature is almost evenly distributed on the plane 0.8 nm above the surface where the C_{60} molecule is placed due to the high conductivity of the graphene. Therefore, the force due to the thermal gradient ($\mathbf{F}_{thermal}$) is negligible due to the small thermal gradient, small size of the C_{60} molecule and the vacuum environment. As a low-loss plasmonic material, the plasmon properties can be manipulated via electrostatic doping. In general, the coulomb force on the insulator is small. Hence, the coulomb force on the C_{60} nanoparticle can be safety omitted.

Adding the response from the optical force ($\mathbf{F}_{opt}$) into the Langevin dynamics, we could tailor the overall interaction potential and use it to control nanoparticles adsorbed on graphene. A series of simulations were performed assuming a static stable trap at $E_F = 0.32$ eV and randomly placing a series of fullerene C_{60} molecule at various locations on the nanoconveyor under different incident intensities. The simulation results (details in Section S5 of the Supporting Information) show that the physisorbed C_{60} admolecule could be trapped into the optical potential well within a timeframe of 20 ns. The escape-velocity threshold is also calculated (details in Section S6 of the Supporting Information) to demonstrated this prediction.

In order to demonstrate the flexibility of the designed structure for controlling the position of the nanoparticle, we apply a time-varying stair-case function to the Fermi level $E_F(t)$ in the inset of **Figure 4**a. The Fermi level of the graphene sheet is changed from 0.32 to 0.27 eV in a stepwise function, each step lasting 10 ns. As can be seen from Figure 4a, the Langevin dynamic simulations show that this proposed function can be applied to transfer the nanoparticle from one end of the structure to the other. The trajectory of the nanoparticle in the inset of Figure 4a shows that this movement has a smooth transition. Figure 4b presents a statistical analysis of the particle position, showing the probability of the location for the nanoparticle for each step. $E_F(t)$ corresponds to the backgate voltage screening the graphene sheet and can be arbitrarily designed, and for example, an average speed of about 10 m s^{-1} is obtained in the case presented in Figure4b. One could readily extend this concept and envision advanced manipulation of the speed and even acceleration of nanoparticles, in addition to electrically controllable amplitude and direction of optical force exerted on the nanoparticles.

In summary, here we propose a novel mechanism for a sub-nm molecule transportation platform (stable trapping and electrically configurable conveying). One can easily devise different time varying voltage functions applied on a single back gate to control the speed, location and acceleration of a sub-1 nm particle along the graphene nanoconveyor. This concept can be widely

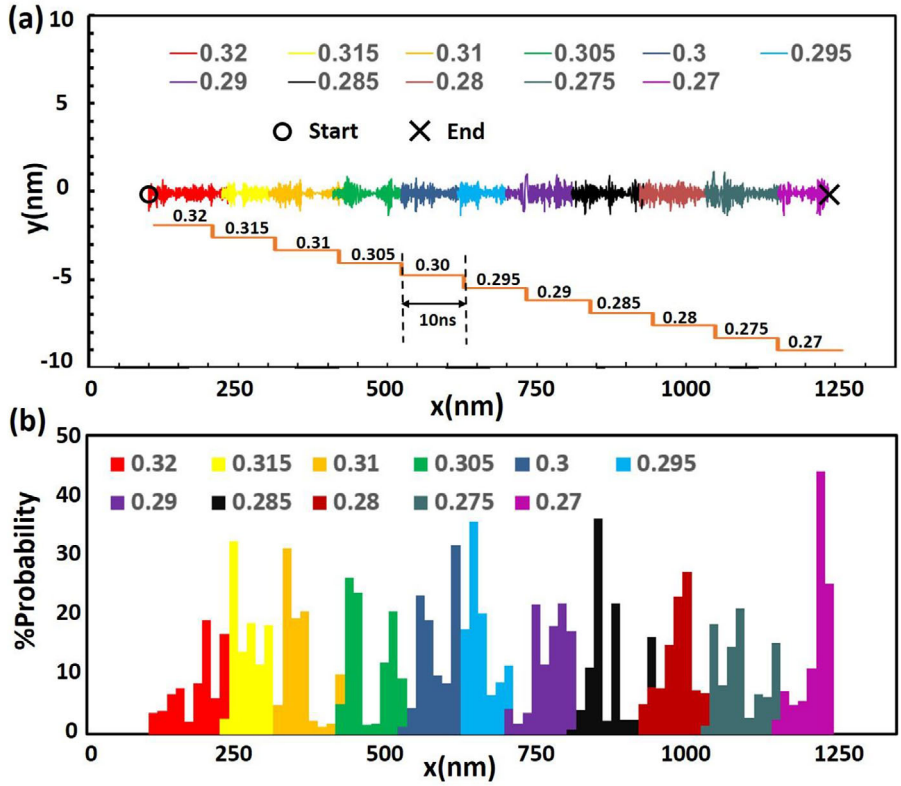

Figure 4. Time domain transfer dynamics of Fullerene C_{60} across graphene nanoconveyor. a) Trajectory of a nanoparticle placed on one edge under a staircase function changing its Fermi level using electrostatic doping. $E_F(t)$ is plotted in the inset graph. b) Nanoparticle position probability distribution versus Fermi level. The incident intensity is 250 mW μm^{-2}.

adopted to design a plethora of structures using graphene plasmons, as versatile platforms for advanced particle nanomanipulation. This conceptual proposal opens a new dimension particularly in nanoparticle manipulation and may lead to many exciting applications in future lab-on-chip nanotechnology.

Supporting Information

Supporting Information is available from the Wiley Online Library or from the author.

Acknowledgements

C.-W.Q. acknowledges the support from Ministry of Education, Singapore (Grant No. R-263-000-D11-114).

Author Contributions

M.D., M.J.Z., and T.Z. contributed equally to this work. C.-W.Q. conceived the idea and supervised the work. M.D., X.Z., Z.L., and M.Q. designed the simulation experiments, M.J.Z., B.G., Q.B., and S.M. carried out the theoretical modeling. T.Z., J.-S.L., and A.T.S.W. contributed to the analysis. All authors contributed significantly to the discussion of results and the preparation of the manuscript.

Conflict of Interest

The authors declare no conflict of interest.

Keywords

Fermi level, graphene, nanoplasmonic tweezers, optical force

Received: January 31, 2020
Revised: May 14, 2020
Published online: July 2, 2020

[1] J. Lu, H. Yang, L. Zhou, Y. Yang, S. Luo, Q. Li, M. Qiu, *Phys. Rev. Lett.* **2017**, *118*, 043601.
[2] V. Shvedov, A. R. Davoyan, C. Hnatovsky, N. Engheta, W. Krolikowski, *Nat. Photonics* **2014**, *8*, 846.
[3] A. Ashkin, *Phys. Rev. Lett.* **1970**, *24*, 156.
[4] A. Ashkin, J. M. Dziedzic, J. Bjorkholm, S. Chu, *Opt. Lett.* **1986**, *11*, 288.
[5] S. Chu, J. E. Bjorkholm, A. Ashkin, A. Cable, *Phys. Rev. Lett.* **1986**, *57*, 314.
[6] A. Ashkin J. Dziedzic, *Proc. Natl. Acad. Sci. USA* **1989**, *86*, 7914.
[7] A. Ashkin J. M. Dziedzic, *Science* **1987**, *235*, 1517.
[8] H. Lüddens, D. B. Pritchett, M. Köhler, I. Killisch, K. Keinänen, H. Monyer, R. Sprengel, P. H. Seeburg, *Nature* **1990**, *346*, 648.

[9] P. J. Pauzauskie, A. Radenovic, E. Trepagnier, H. Shroff, P. Yang, J. Liphardt, *Nat. Mater.* **2006**, *5*, 97.
[10] R. Agarwal, K. Ladavac, Y. Roichman, G. Yu, C. M. Lieber, D. G. Grier, *Opt. Express* **2005**, *13*, 8906.
[11] A. Dogariu, S. Sukhov, J. Sáenz, *Nat. Photonics* **2013**, *7*, 24.
[12] J. Chen, J. Ng, Z. F. Lin, C. T. Chan, *Nat. Photonics* **2011**, *5*, 531.
[13] A. Novitsky, C. W. Qiu, H. F. Wang, *Phys. Rev. Lett.* **2011**, *107*, 203601.
[14] A. Novitsky, C.-W. Qiu, A. Lavrinenko, *Phys. Rev. Lett.* **2012**, *109*, 023902.
[15] D. G. Grier, *Nature* **2003**, *424*, 810.
[16] A. N. Grigorenko, N. W. Roberts, M. R. Dickinson, Y. Zhang, *Nat. Photonics* **2008**, *2*, 365.
[17] L. Novotny, R. X. Bian, X. S. Xie, *Phys. Rev. Lett.* **1997**, *79*, 645.
[18] M. L. Juan, M. Righini, R. Quidant, *Nat. Photonics* **2011**, *5*, 349.
[19] H. Raether, *Surface Plasmons on Smooth and Rough Surfaces and On Gratings*, Springer, Berlin **1988**, p. 91.
[20] M. Righini, P. Ghenuche, S. Cherukulappurath, V. Myroshnychenko, F. J. García de Abajo, R. Quidant, *Nano Lett.* **2009**, *9*, 3387.
[21] K. Wang, E. Schonbrun, P. Steinvurzel, K. B. Crozier, *Nat. Commun.* **2011**, *2*, 469.
[22] C. Chen, M. L. Juan, Y. Li, G. Maes, G. Borghs, P. Van Dorpe, R. Quidant, *Nano Lett.* **2012**, *12*, 125.
[23] Y. Pang, R. Gordon, *Nano Lett.* **2011**, *11*, 3763.
[24] A. H. Yang, T. Lerdsuchatawanich, D. Erickson, *Nano Lett.* **2009**, *9*, 118.
[25] X. Yang, Y. Liu, R. F. Oulton, X. Yin, X. Zhang, *Nano Lett.* **2011**, *11*, 321.
[26] J. Zhang, W. Liu, Z. Zhu, X. Yuan, S. Qin, *Sci. Rep.* **2016**, *6*, 38086.
[27] A. Barik, X. Chen, S.-H. Oh, *Nano Lett.* **2016**, *16*, 6317.
[28] A. A. Saleh J. A. Dionne, *Nano Lett.* **2012**, *12*, 5581.
[29] B. Roxworthy, K. Ko, A. Kumar, K. Fung, E. Chow, *Nano Lett.* **2012**, *12*, 796.
[30] Z. Li, S. Zhang, L. Tong, P. Wang, B. Dong, H. Xu, *ACS Nano* **2014**, *8*, 701.
[31] H. Chen, S. Liu, J. Zi, Z. Lin, *ACS Nano* **2015**, *9*, 1926.
[32] Y. Shi, S. Xiong, L. K. Chin, J. Zhang, W. Ser, J. Wu, T. Chen, Z. Yang, Y. Hao, L. Bo, H. Y. Peng, P. T. Din, C. W. Qiu, A. Q. Liu, *Sci. Adv.* **2018**, *4*, eaao0773.
[33] P. Hansen, Y. Zheng, J. Ryan, L. Hesselink, *Nano Lett.* **2014**, *14*, 2965.
[34] Y. Zheng, J. Ryan, P. Hansen, Y.-T. Cheng, T.-J. Lu, L. Hesselink, *Nano Lett.* **2014**, *14*, 2971.
[35] O. Brzobohatý, V. Karásek, M. Šiler, L. Chvátal, T. Čižmár, P. Zemánek, *Nat. Photonics* **2013**, *7*, 123.
[36] D. B. Ruffner, D. G. Grier, *Phys. Rev. Lett.* **2012**, *109*, 163903.
[37] L. Paterson, M. P. MacDonald, J. Arlt, W. Sibbett, P. E. Bryant, K. Dholakia, *Science* **2001**, *292*, 912.
[38] M. Geiselmann, R. Marty, J. Renger, F. J. García de Abajo, R. Quidant, *Nano Lett.* **2014**, *14*, 1520.
[39] Y. Z. Shi, S. Xiong, Y. Zhang, L. K. Chin, Y. –Y. Chen, J. B. Zhang, T. H. Zhang, W. Ser, A. Larrson, S. H. Lim, J. H. Wu, T. N. Chen, Z. C. Yang, Y. L. Hao, B. Liedberg, P. H. Yap, K. Wang, D. P. Tsai, C.-W. Qiu, A. Q. Liu, *Nat. Commun.* **2018**, *9*, 815.
[40] L. Tong, V. D. Miljković, M. Käll, *Nano Lett.* **2010**, *10*, 268.
[41] T. Cao, J. Bao, L. Mao, T. Zhang, A. Novitsky, M. Nieto-Vesperinas, C.-W. Qiu, *ACS Photonics* **2016**, *3*, 1934.
[42] A. N. Grigorenko, M. Polini, K. S. Novoselov, *Nat. Photonics* **2012**, *6*, 749.
[43] F. H. L. Koppens, D. E. Chang, F. J. García de Abajo, *Nano Lett.* **2011**, *11*, 3370.
[44] Z. Fei, G. O. Andreev, W. Bao, L. M. Zhang, A. S. McLeod, C. Wang, M. K. Stewart, Z. Zhao, G. Dominguez, M. Thiemens, M. M. Fogler, M. J. Tauber, A. H. Castro-Neto, C. N Lau, F. Keilmann, D. N. Basov, *Nano Lett.* **2011**, *11*, 4701.
[45] J. Chen, M. Badioli, P. Alonso-González, S. Thongrattanasiri, F. Huth, J. Osmond, M. Spasenović, A. Centeno, A. Pesquera, P. Godignon, A. Z. Elorza, N. Camara, F. J. G. de Abajo, R. Hillenbrand, F. H. L. Koppens, *Nature* **2012**, *487*, 77.
[46] Z. Fei, A. S. Rodin, G. O. Andreev, W. Bao, A. S. McLeod, M. Wagner, L. M. Zhang, Z. Zhao, M. Thiemens, G. Dominguez, M. M. Fogler, A. H. Castro Neto, C. N. Lau, F. Keilmann, D. N. Basov, *Nature* **2012**, *487*, 82.
[47] V. W. Brar, M. S. Jang, M. Sherrott, J. J. Lopez, H. A. Atwater, *Nano Lett.* **2013**, *13*, 2541.
[48] E. H. Hwang, S. Das Sarma, *Phys. Rev. B* **2007**, *75*, 205418.
[49] B. Wunsch, T. Stauber, F. Sols, F. Guinea, *New J. Phys.* **2006**, *8*, 318.
[50] S. H. Mousavi, P. T. Rakich, Z. Wang, *ACS Photonics* **2014**, *1*, 1107.
[51] W. Lu, H. Chen, S. Liu, J. Zi, Z. Lin, *Phys. Chem. Chem. Phys.* **2016**, *18*, 8561.
[52] B. Zhu, G. Ren, Y. Gao, Y. Yang, M. J. Cryan, S. Jian, *IEEE Photonics Technol. Lett.* **2015**, *27*, 891.
[53] J.-D. Kim, Y.-G. Lee, *Carbon* **2016**, *103*, 281.
[54] M. Jafary-Zadeh, C. D. Reddy, Y. W. Zhang, *Phys. Chem. Chem. Phys.* **2014**, *16*, 2129..
[55] A. J. Martínez-Galera, J. M. Gómez-Rodríguez, *J. Phys. Chem. C* **2011**, *115*, 23036.
[56] A. J. Oyer, J.-M. Y. Carrillo, C. C. Hire, H. C. Schniepp, A. D. Asandei, A. V. Dobrynin, D. H. Adamson, *J. Am. Chem. Soc.* **2012**, *134*, 5018.
[57] E. I. Altman, R. J. Colton, *Surf. Sci.* **1993**, *295*, 13.
[58] P. A. Gravil, M. Devel, P. Lambin, X. Bouju, C. Girard, A. A. Lucas, *Phys. Rev. B* **1996**, *53*, 1622.
[59] M. Jafary-Zadeh, C. D. Reddy, Y.-W. Zhang, *Phys. Chem. Chem. Phys.* **2012**, *14*, 10533.
[60] M. Jafary-Zadeh, Y.-W. Zhang, *Sci. Rep.* **2015**, *5*, 12848.
[61] T. Sato, N. Iwahara, N. Haruta, K. Tanaka, *Chem. Phys. Lett.* **2012**, *531*, 257.
[62] T. Gilberto, Z. Francesco, *Small* **2007**, *3*, 1694.
[63] J. A. Izaguirre, D. P. Catarello, J. M. Wozniak, R. D. Skeel, *J. Chem. Phys.* **2001**, *114*, 2090.
[64] R. W. Pastor, B. R. Brooks, A. Szabo, *Mol. Phys.* **1988**, *65*, 1409.
[65] T. Ala-Nissila, R. Ferrando, S. C. Ying, *Adv. Phys.* **2002**, *51*, 949.
[66] J. Chen, M. Badioli, P. Alonso-González, S. Thongrattanasiri, F. Huth, J. Osmond, M. Spasenovic, A. Centeno, A. Pesquera, P. Godignon, A. Zurutuza, N. Camara, J. G. de Abajo, R. Hillenbrand, F. Koppens, *Nature* **2012**, *487*, 77.
[67] M. Jafary-Zadeh, C. D. Reddy, V. Sorkin, Y.-W. Zhang, *Nanoscale Res. Lett.* **2012**, *7*, 148.
[68] H. Hedgeland, P. Fouquet, A. P. Jardine, G. Alexandrowicz, W. Allison, J. Ellis, *Nat. Phys.* **2009**, *5*, 561.
[69] H.-R. Jiang, H. Wada, N. Yoshinaga, M. Sano, *Phys. Rev. Lett.* **2009**, *102*, 208301.
[70] R. L. Saxton, W. E. Ranz, *J. Appl. Phys.* **1952**, *23*, 917.
[71] J. C. Ndukaife, A. V. Kildishev, A. G. A. Nnanna, V. M. Shalaev, S. T. Wereley, A. Boltasseva, *Nat. Nanotechnol.* **2016**, *11*, 53.